The Influence of TiN, ZrN and $Ti_xZr_{1-x}N$ Layers of Anti-friction Multi-layer Coatings on Corrosion Resistance of Hard Alloy in Sodium Hydroxide Solution

AL Kameneva*

Perm National Research Polytechnic University, Department of Innovative Engineering Technology, Komsomol'skii pr. 29, Perm, 614990, Russia.

ABSTRACT

The influence of the sequence and deposition method of TiN, ZrN and Tix Zr1-xN layers of multi-layer coatings with respect to the corrosion resistance of hard alloy in sodium hydroxide solution has been studied by electrochemical methods (polarization and impedance measurements) and optical microscopy. It is shown that various corrosion resistance of multi-layer coatings is caused by surface defects and internal defects of the coating layers as well as differences in the oxygen adsorption on the coatings surface in 5% solution of NaOH (without de-aerating) and, consequently, differences in the adsorption of intermediates and differences in the rate constants of charge transfer.

Keywords: multi-layer coatings, TiN, ZrN and $Ti_xZr_{1-x}N$ layers, corrosion resistance, impedance, 5% solution of NaOH

*Corresponding author

INTRODUCTION

The wear of the cutting carbide plates, working in conditions of dry friction and impact of alkaline and acidic environments is caused by the low corrosive properties and tribological properties, such as wear and friction resistance, of carbide plates [1-4]. Processing of most materials in all cases is determined by the state of the most loaded surface layer. The special coatings with complex functional properties are used to improve a efficiency of the cutting carbide plates. TiN multilayer coatings still play an important role. However, ZrN, $Ti_xZr_{1-x}N$, $Ti_{1-x}Al_xN$, and $Cr_{1-x}Al_xN$ multi-layer coatings have a greater hardness and greater oxidation resistance [5-11].

However, the influence patterns of the sequence and deposition method of TiN, ZrN and $Ti_xZr_{1-x}N$ layers of multi-layer coatings with respect to the corrosion resistance of hard alloy have not been studied to a sufficient extent.

This paper examines the corrosion resistance of hard alloy with a multilayer coating of TiN, ZrN and $Ti_xZr_{1-x}N$ repetitive layers applied by magnetron sputtering (MS), cathodic arc evaporation (CAE) or by a combined method in 5% solution of NaOH. Corrosion resistance of multi-layer coatings was compared with that of single-layer coating TiN and ZrN coatings.

EXPERIMENTAL

Multi-layer coatings with TiN, ZrN and $Ti_xZr_{1-x}N$ repetitive layers on test samples made of solid alloys VK8 were deposited on a URM3.279.048 unit with two cathodic arc evaporators and four magnetron sprayers. Substrate preparation: the surface of all cutting plates from solid alloys VK8 (substrate), were subjected to the ion cleaning and heating procedure using one cathodic arc evaporator with titanium cathode. The multi-layer coatings adhesion was done by depositing the Ti or TiZr interlayer between substrate and first layer and by carrying out ion bombardment of intermediate TiZr layers. The thickness of the Ti and TiZr interlayers varies from 100 to 500 nm. The alternate or simultaneous operation of the cathodic arc evaporator and magnetron sprayer was used for receiving of the multi-layer coatings with different layer thickness, compositional gradients, and depth positions of different elements and properties of the multi-layer coatings ultimately. Examples of using different methods for depositing multi-layer coatings:

Structure (1): The multi-layer coating TiZr-*$Ti_xZr_{1-x}N$-TiZr*-$Ti_xZr_{1-x}N$ [12] is produced by cathodic arc evaporation. The intermediate TiZr layer and intermediate $Ti_xZr_{1-x}N$ layer are repeated from two to four times on the TiZr interlayer. The re-TiZr layer is deposited on the re-$Ti_xZr_{1-x}N$ layer to obtain a hardness gradient, effectively inhibit crack propagation at the boundary layers and to increase the thermodynamic stability. The top layer of multi-layer coating is $Ti_xZr_{1-x}N$ layer. The thickness of re-$Ti_xZr_{1-x}N$ layer, re-TiZr layer, and top $Ti_xZr_{1-x}N$ layer is 1.0 µm, 10 nm, and 1.0 µm, respectively.

Structure (2): The method for deposition of the multi-layer coating Ti-*TiN-ZrN*-$Ti_xZr_{1-x}N$ is varied to be either magnetron sputtering, cathodic arc evaporation or combined method, i.e., the simultaneous usage of the cathodic arc evaporator and magnetron sprayer [13]. The intermediate TiN layer is deposited on the Ti interlayer produced by magnetron sputtering and on the top of this TiN magnetron sputtered layer is deposited intermediate ZrN layer by cathodic arc evaporation. These intermediate TiN layer and intermediate ZrN layer are repeated from two to four times. The top $Ti_xZr_{1-x}N$ layer of multi-layer coating is carried out simultaneously. The thickness of re-TiN layer, re-ZrN layer, and top $Ti_xZr_{1-x}N$ layer is 400 nm, 1.3 µm, and 2.0 µm, respectively.

Structure (3): The method for deposition of the multi-layer coating Ti-*TiN–$Ti_xZr_{1-x}N$*-$Ti_xZr_{1-x}N$ is varied to be either magnetron sputtering, cathodic arc evaporation or combined method [14]. The intermediate TiN layer is deposited on the Ti interlayer produced by cathodic arc evaporation and on the top of this TiN magnetron sputtered layer is deposited intermediate $Ti_xZr_{1-x}N$ layer by simultaneous operation of the cathodic arc evaporator and magnetron sprayer. These intermediate TiN layer and intermediate $Ti_xZr_{1-x}N$ layer are repeated from two to four times. The deposition of the top $Ti_xZr_{1-x}N$ layer is carried out simultaneously. The thickness of re-TiN layer, re-$Ti_xZr_{1-x}N$ layer, and top $Ti_xZr_{1-x}N$ layer is 300 nm, 1.0 µm, and 1.0 µm, respectively.

Structure (4): The multi-layer coating Ti-TiN-*Zr-ZrN*-Zr-*Ti$_x$Zr$_{1-x}$N-Zr*-Ti$_x$Zr$_{1-x}$N is produced by magnetron sputtering [15]. The second TiN interlayer is deposited on the first Ti interlayer and on the top of this TiN interlayer is deposited intermediate Zr layer. On the top of this intermediate Zr layer is deposited intermediate ZrN layer. These intermediate Zr layer and the intermediate ZrN layer are repeated twice. The next intermediate Ti$_x$Zr$_{1-x}$N layer is deposited on Zr layer and on the top of this Ti$_x$Zr$_{1-x}$N layer is deposited intermediate Zr layer. The intermediate Ti$_x$Zr$_{1-x}$N layer and intermediate Zr layer are repeated twice. The top layer of multi-layer coating is Ti$_x$Zr$_{1-x}$N layer. The thickness of the all coating layers is 200 nm.

A total Ti$_x$Zr$_{1-x}$N thin film thickness is 3.0–5.0 μm. The thickness of coating layers was determined from a field emission electron microscope Ultra 55 with EDX attachments and resolution of the secondary electrons up to 1 nm at 15 kV.

The coated samples (electrodes) submitted for electrochemical measurements were potted in epoxy in such a way as to leave exposed only one surface of each coated sample (0.65 cm^2). Surface electrodes are purified ethanol and washed in the working solution.

Polarization and impedance measurements of VK8 with the multi-layer coatings were taken at room temperature (295 - 297 K) inside a three-electrode cell filled with unstirred solution of 5% NaOH without deaerating. An «open-circuit-potential/time» curve was built for each sample steeped in solution. The impedance spectrum was measured at fixed intervals (100 minutes) of time, in the *f* frequency range from 30 kHz to 0,003 Hz, so long as the corrosion potential E$_{cor}$ not reached a constant value. In the next step the impedance was measured at a number of anodic polarization in the frequency range from 10 kHz to 0.01 Hz (10 points per decade). The amplitude of the ac signal was 10 μV, the duration of the stabilization of the current at each potential before the measurement of the impedance spectrum was 10 min.

Electrochemical measurements were performed in a divided cell with the anodic and cathodic compartments. The impedance was measured on Solartron 1255 frequency analyzer and potentiostat Solartron 1287 (Solartron Analytical). The CorrWare, ZPlot, CorrView and ZView programs were used for the measurements and data processing. The electrode potentials *E* were measured relative to the standard hydrogen electrode (st.h.e.).

Morphological features of the multi-layer coatings (1-4) before and after the corrosion tests were studied using universal metallographic microscope Altami MET5 with software.

Corrosion resistance of multi-layer coatings (1-4) [12-15] was compared with that of single-layer TiN and ZrN coatings [8-11] formed without variation of the plasma source and the composition during deposition.

The influence of the layer composition of multi-layer coatings on corrosion resistance of hard alloy in sodium hydroxide solution was assessed by the optimum combination of corrosion properties of the solid alloy with multi-layer coatings.

RESULTS AND DISCUSSION

Stationary values of corrosion potentials for multi-layer coatings (1-4) were -0.13 V, -0.10 V, -0.38 V, and -0.12 V, respectively. Figure 1 shows the anodic polarization curves (Fig. 1). All anodic polarization curves for the multi-layer coatings (1-4) are of the same type: for small polarizations observed areas with high slope, at higher polarizations observed Tafel slope according to dE / dlgi = 0.16 − 0.18 ln (i - current density), with the further increase of polarization appear deviations from Tafel curves.
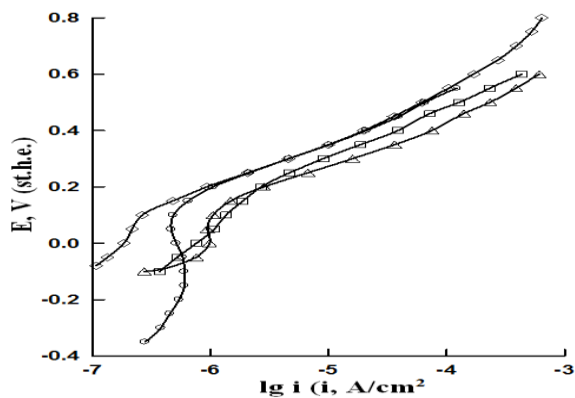
Figure 1: Anodic polarization curves of the hard alloy VK8 with multi-layer coatings with the following structures: (1) □; (2) ◊; (3) o; (4) Δ

Figure 2 shows the impedance plots for electrodes with multi-layer coatings at constant E_{cor}. The impedance plots in the complex plane have the form of semicircles with an off-axis under Z' center for the multi-layer coatings, except structure (3) [14].
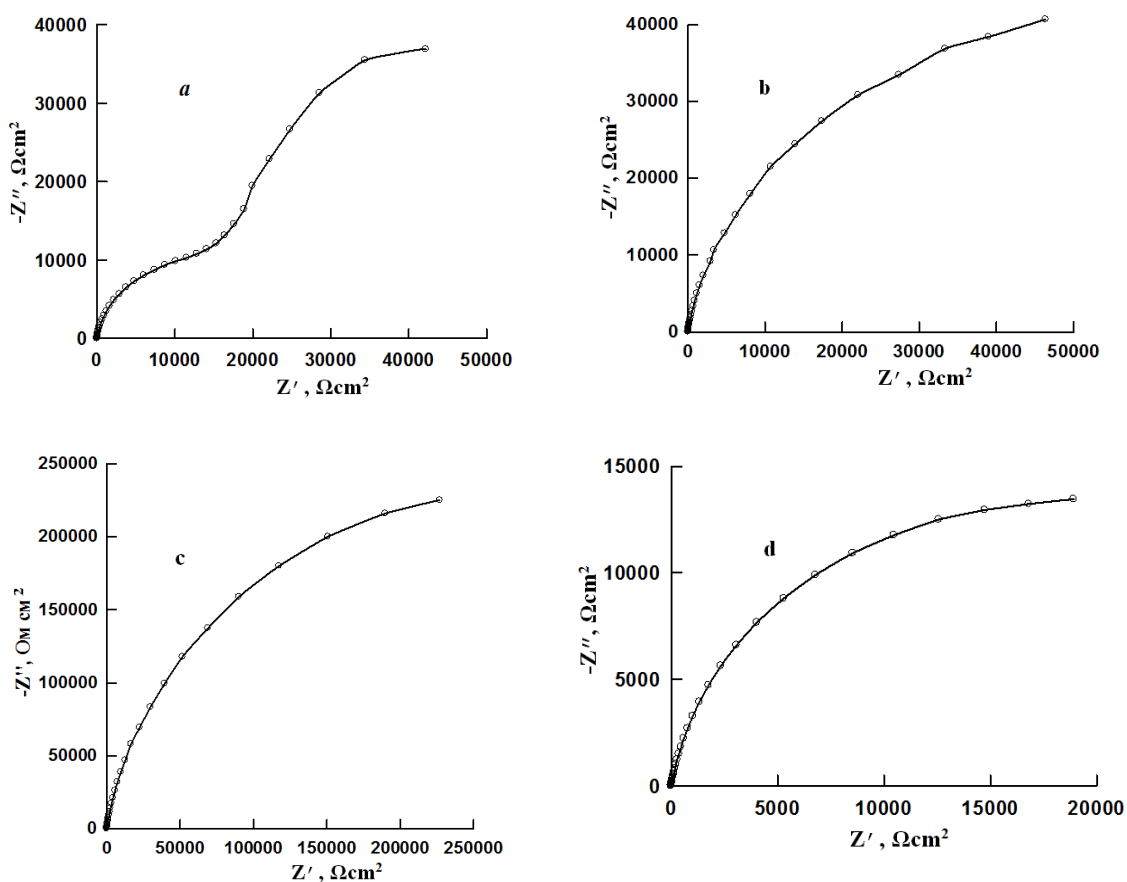

Figure 2: Nyquist plots at constant E_{cor} for multi-layer coatings: a) (3); b) (1); c) (2); d) (4).
Z' and Z'' - real and imaginary components of the impedance

Approximation of the impedance plots close to the semicircle allowed us to determine the low-frequency limit of the impedance or polarization resistance Rp (Table 1), which is a measure of the corrosion rate [15]. The decline rate of R_p depends on the deposition process conditions and structure of the multi-layer coatings. Impedance data are in qualitative agreement with the results of polarization measurements (Tab.1, Fig.1). The multi-layer coating (2) has the highest value of R_p and the lowest value of corrosion current density i_{cor}. The multi-layer coating (4) shows the lowest value of R_p and the highest value of i_{cor}. Corrosion properties of multi-layer coatings were compared with that of single-layer TiN coating and ZrN coating formed without variation of the plasma source and the composition during deposition process [8-11] (Tab.1).
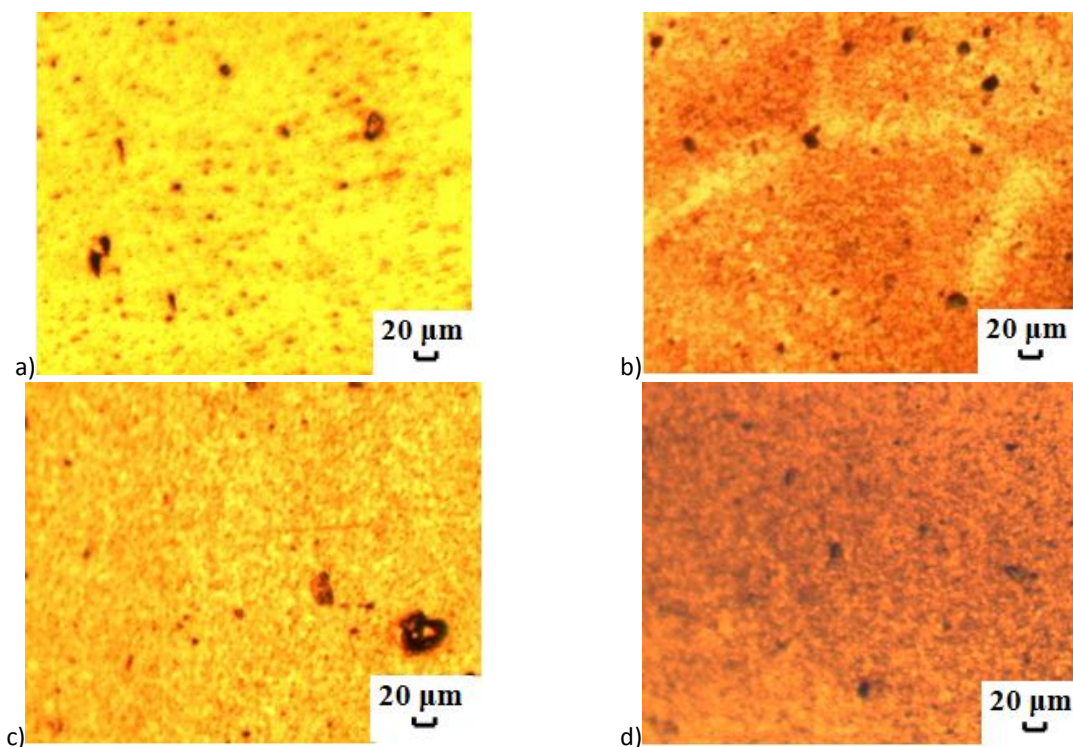
Table 1: The results of corrosion tests

Corrosion properties of the multi-layer coating	Structure of multi-layer coating				ZrN MS [8]	ZrN CAE [9]	TiN MS [10]	TiN CAE [11]
	(1) [12]	(2) [13]	(3) [14]	(4) [15]				
$R_p, \cdot10^5 \Omega cm^2$	1,1	5,5	1,0	0,3	0,7	12	0,03	33
$i_{cor}, \cdot10^{-7} A/cm^2$	3,6	2,0	5,5	10	7,2	-	70	2,3

High values of R_p and minimum values of i_{cor} ($i_{cor} \leq 10^{-6}$ A/cm^2) indicate a high corrosion resistance of studied multi-layer coatings with high strength of crystal lattices [16, 17].

The composition and method for deposition of the top layer are not a major cause of significant differences in the values of R_p and i_{cor} because the composition and the deposition method of the top layer of multilayer coatings (2) and (3) are identical.

The highest value of R_p and the lowest value of i_{cor} correspond to multi-layer coating (2) with a maximum thickness of the intermediate layer and its top layer. In the first approximation, we can speak of a relationship between the layer thickness of the multi-layer coating and its corrosion rate: the higher the layer thickness, the higher the corrosion resistance of the coating as a whole.
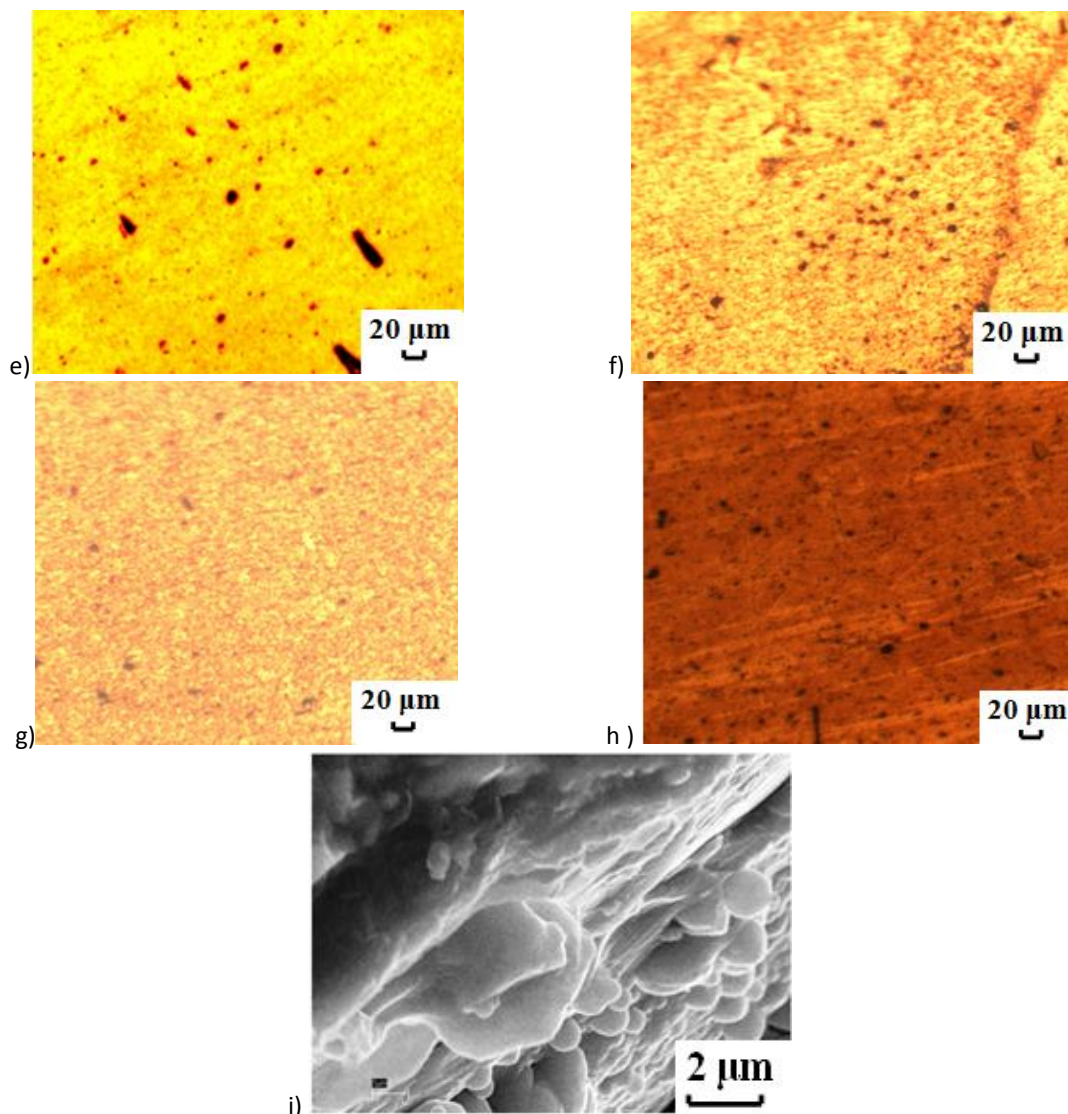
Figure 3: The surface morphology of multi-layer coating: a, b - (1); c, d - (2); e, f - (3); g, h – (4); a, c, e, g - before corrosion tests; b, d, f, h - after corrosion tests

The local discontinuities of top layer of the multi-layer coatings are the other reason for the change in i_{cor} and R_p. Nature and extent of the defeat of the multi-layer coatings in a solution of 5% NaOH during anodic polarization differs insignificantly (Fig. 3). A slight dissolution of the top layer of multi-layer coatings is prevails over a large area, more conspicuous in multi-layer coatings (3) and (4). Coating (4) shows the highest dissolution in some areas (Fig. 3, h). The deterioration of corrosion resistance of coating (4) were caused by the metal droplet on the surface and within the multi-layer coating (Fig. 3, i). It is established that change of the true surface area of the samples with coatings is not the primary cause of the change in the value of R_p. For example, the value of the capacitance C of the coatings (2) and (4) differ in 3 times when E = 0, whereas the value of R_p coatings (2) and (4) differ in 18 times at E_{cor} (Fig. 4).

The difference of the phase composition of the layers [11] is the probable cause of changing of adsorption of oxygen which inhibitory electrode processes at the multi-layer coating surface in the electrolyte solution. Chemisorption of oxygen causes an increase of the activation energy of the electrode process, which in turn leads to a significant reduction in the constants of the charge transfer rate due to the exponential functional relation between the activation energy and rate constant. The correlation between the corrosion resistance of the multi-

layer coating and the value of the differential capacitance C of the electrode with the multi-layer coating is the result of oxygen chemisorption (Fig. 4). The inverse proportionality between C and R_p is absent.

The differential capacitance values (Fig. 4) are not typical for electrodes with phase oxide layers, so the two partially overlapping semicircles (Fig. 2, a) are not associated with the presence of an oxide layer on the surface of the coated sample (3).
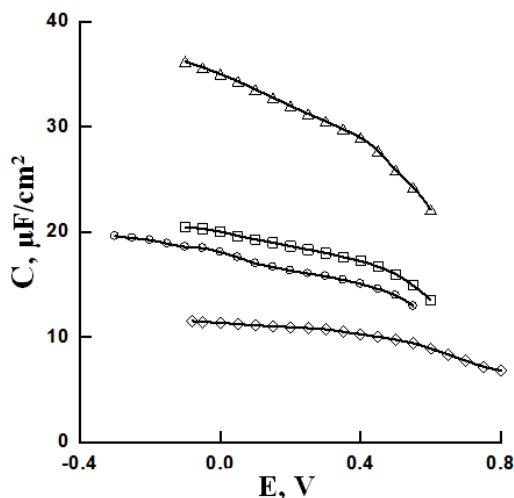

Figure 4: Differential capacitance curves for multi-layer coatings:
(1) □; (2) ◊; (3) o; (4) Δ. (f=10 kHz)

The impedance at various points of the anodic potentiostatic polarization curves was measured for a more complete characterization of the corrosion resistance of the multi-layer coatings (2) and (4) with the highest and lowest value of R_p, respectively. In the case of a multi-layer coating (2) the impedance plots retain a simple form up to E = 0.6 V (Fig. 5-7). For example, with the increase of electrode potential at E> 0 the value of the impedance is reduced, when at E ≥ 0.7 the form of impedance plots is complicated: three peaks are distinguishable on the Bode plot (Fig. 8).
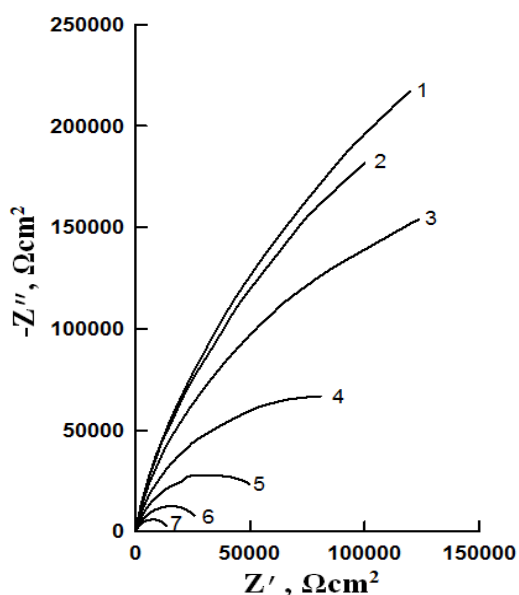

Figure 5: Nyquist plots for multi-layer coating (2). The electrode potential *E*:
1 − 0; 2 − 0.05 V; 3 − 0.1 V; 4 − 0.15 V; 5 − 0.2 V; 6 − 0.25 V; 7 − 0.3 V
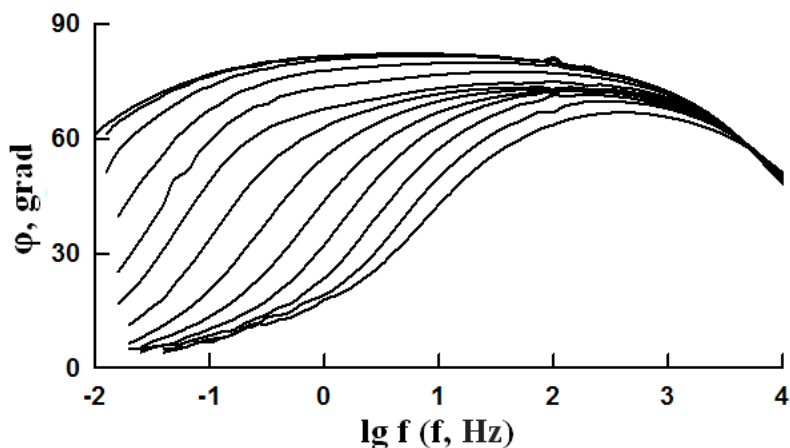
Figure 6: Bode plots for multi-layer coating (2). The curves from top to bottom correspond to E from 0 to 0.6 V in steps of 0.05 V. φ - phase angle of the impedance, f – frequency
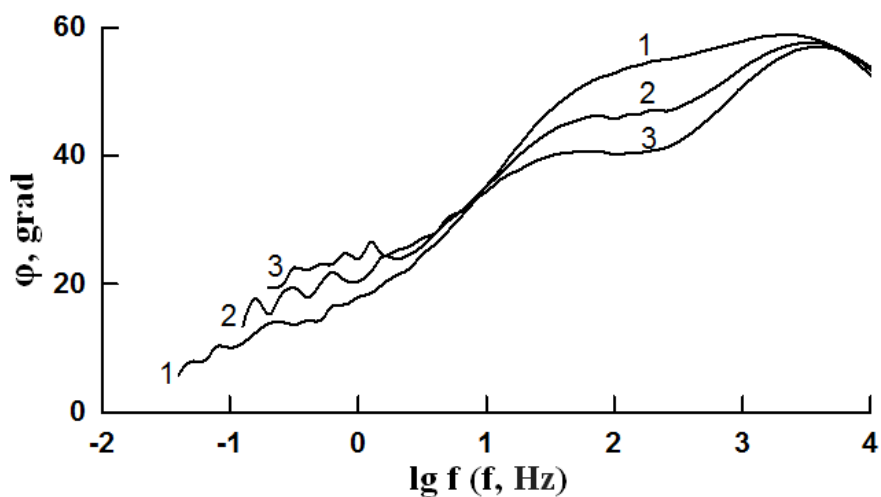

**Figure 7: Bode plots for multi-layer coating (2).
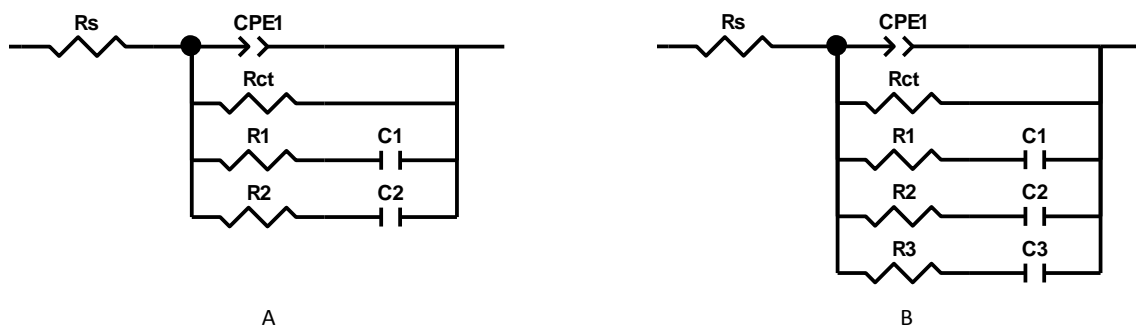The electrode potential *E*: 1 – 0.7 V; 2 – 0.75 V; 3 – 0.8 V**

Figure 8: Equivalent electrical circuit: R_s – solution resistance, CPE1- constant phase element, simulating the electrical double layer at the electrode / solution boundary (admittance of the CPE is $Y_{CPE} = Q(j\omega)^p$, where p – parameter, which characterizes the phase angle CPE ($0 < p < 1$, Q – coefficient, R_{ct} – charge transfer resistance). Elements of R_i and C_i (i = 1, 2, 3) describe the relaxation of the adsorption of intermediates in the imposition of a sinusoidal signal of small amplitude

It has been established that the impedance properties of the multi-layer coating (2) are similar to the impedance properties of the ZrN coating, deposited by CAE [8]. The equivalent circuits from [8] were used to describe the impedance of the electrodes with multi-layer coatings (Figure 8). The equivalent circuit A (Fig. 8) is model of interface boundary where in the absence of the influence of diffusion processes takes place electrode reaction of two intermediate adsorbed substances. The electrode reaction for circuit A flows in three successive stages [17]. The equivalent circuit B - model of interface boundary where in the absence of the influence of diffusion processes takes place intermediate electrode reaction of three adsorbed substances. The electrode reaction for circuit B flows in four successive stages (Fig. 8).

The equivalent circuit B (Fig. 8) satisfactorily describes the experimental plots of impedance for the sample with multi-coating (2) (Fig.9). The sum of the squared deviations of the estimated and experimental values of the Z' and Z'' is 0.023. The error of determination of the values of all parameters is less than 10%. The equivalent circuit A noticeably worse describes the experimental data for this sample: the sum of the squared deviations equal of 0.081. The impedance data for the electrodes VK8 with multi-layer coatings in the solution of 5% NaOH satisfactorily describes by the multi-step anodic process occurring on the surface of the coating at the limiting stage of the charge transfer. A similar conclusion was obtained earlier for TiN and ZrN coatings [8].
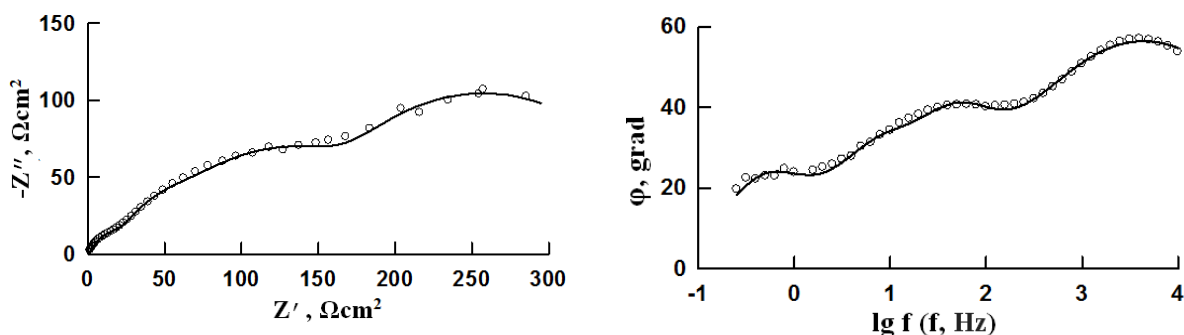

Figure 9: Experimental impedance plots (points) for the multi-layer coating (2) at E = 0.8 V, and calculated impedance plots for the equivalent circuit B (lines) which is the closest to the experimental

Figure 10 shows the two overlapping peaks at the Bode plots in a wide range of potentials and Figure 11 shows the three overlapping arcs at the Nyquist plots at the highest potentials. Therefore circuit A (Figure 8), corresponding to the multistage process, was used to quantify the impedance data for the sample with multi-layer coating (4) with the least corrosion resistance.

Based on the similarity of anodic polarization processes in the solution of 5% NaOH for the sample (2) with highest corrosion resistance and for the sample (4) with lowest corrosion resistance, we can be concluded that the difference in the properties of multi-layer coatings are mainly due to differences in quantitative values of the constants of stage rate, the adsorption values of intermediates and the like, but not with the difference of the nature processes.
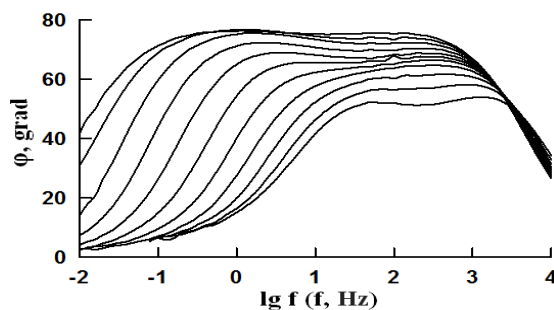

Figure 10: Bode plots for the multi-layer coatings (4). The plots from top to bottom correspond to E from 0.1 V to 0.6 V in steps of 0.05 V
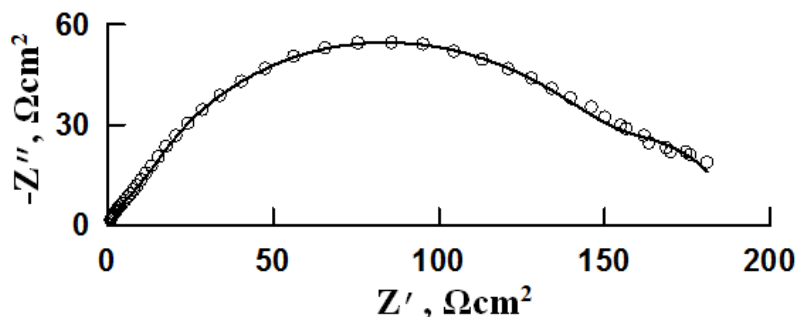
Figure 11: Experimental impedance plot (point) for the multi-layer coating (4) at the electrode potential E = 0.6 V, and calculated impedance plot for the equivalent circuit A which is the closest to the experimental.

CONCLUSION

Correlation between corrosion properties and the deposition method, sequence and composition of layers of multi-layer coatings has been established.

The main cause of various corrosion resistance of multi-layer coatings are the differences in the oxygen adsorption on the coating surface in the 5% solution of NaOH (without deaerating) and, consequently, differences in the rate constants of charge transfer and adsorption of intermediates, as well as surface defects and internal defects of the coatings.

The multi-layer coating Ti-*TiN-ZrN*-$Ti_xZr_{1-x}N$ with the highest corrosion resistance, minimum of the surface defects and internal defects, and thickness of the re-ZrN layer greater than 1 μm is the most effective for corrosion protection of hard alloy in the solution of 5% NaOH. The optimal method for deposition of the re-ZrN layer of the multi-layer coating Ti-*TiN-ZrN*-$Ti_xZr_{1-x}N$ is cathodic arc evaporation.

Multilayer coatings [12-15] with high corrosion properties are able to increase the operational stability of the cutting tool in the mining and oil industry, and other operational purposes.

ACKNOWLEDGEMENTS

REFERENCES

[1]   G.P. Fetisov, M.G. Karpman. Materials science and technology of metals. Moscow; High school, 2000.
[2]   A.L. Kameneva, I.I. Zamaletdinov, et al. Strengthening technology and coating, 5, 11, 2010.
[3]   A.S. Vereshchaka, V.P. Tabakov. Physical basis of the cutting process and cutting tool wear with wear-resistant coatings. Ulyanovsk; UlSTU, 1998.
[4]   V.A. Bondarenko, S.I. Bogoduhov. Quality assurance and improvement in performance of cutting tools. Moscow; Engineering, 2000.
[5]   A.L. Kameneva, V.I. Kichigin, T.O. Soshina, V.V. Karmanov. Using $Ti_{1-x}Al_xN$ coating to enhance corrosion resistance of tool steel in sodium chloride solution, Research Journal of Pharmaceutical, Biological and Chemical Sciences, 2014, 5(5), 1148-1156.
[6]   A.L. Kameneva, V.V. Karmanov, I.V. Dombrovsky. Physical and mechanical properties of $Ti_{1-x}Al_xN$ thin films prepared by different ion-plasma methods, Research Journal of Pharmaceutical, Biological and Chemical Sciences, 2014, 5(6), 762-771.

[7]   A.L. Kameneva. The influence of aluminum on the texture, microstructure, physical, mechanical and tribological properties of $Ti_{1-x}Al_xN$ thin films, Research Journal of Pharmaceutical, Biological and Chemical Sciences, 2014, 5(6), 965-975.

[8]   I.I. Zamaletdinov, V.I. Kichigin, A.L. Kameneva, A.A. Onyanov, A.Y. Klochkov, Corrosion: Materials, protection, 7, 34 (2010).

[9]   I.I. Zamaletdinov, V.I. Kichigin, A.L. Kameneva, A.Y. Klochkov, Corrosion: Materials, protection, 6, 32 (2011).

[10]   I.I. Zamaletdinov, V.I. Kichigin, A.L. Kameneva, A.A. Onyanov, A.Y. Klochkov, Corrosion: Materials, protection, 10, 35 (2011).

[11]   A.L. Kameneva, Corrosion: Materials, protection, 12, 28 (2012).

[12]   Patent 2346078. Russian Federation, 2009.

[13]   Patent 2361013. Russian Federation, 2009.

[14]   Patent 2429311. Russian Federation, 2011.

[15]   Patent 2433209. Russian Federation, 2011.

[16]   W.J. Lorenz, F. Mansfeld, Corrosion Science, 21(9-10), 647, 1981.

[17]   L. Peter, J. Arai, H. Akahoshi, Electroanal. Chem. 482(2), 125, 2000.